

Supporting Information to

## **Cathodic electrochemiluminescence of L012 and its application in antioxidant detection**

Mingqian Tan,<sup>1</sup> Yafeng Wang,<sup>2,3</sup> Ziyong Hong,<sup>4</sup> Ping Zhou,<sup>1</sup> Jie Jiang<sup>4</sup> and Bin Su<sup>\*,1</sup>

<sup>1</sup>Key Laboratory of Excited-State Materials of Zhejiang Province, Department of Chemistry, Zhejiang University, Hangzhou 310058, China

<sup>2</sup>Department of Clinical Laboratory, Sir Run Run Shaw Hospital, School of Medicine, Zhejiang University, Hangzhou 310016, China

<sup>3</sup>Key Laboratory of Precision Medicine in Diagnosis and Monitoring Research of Zhejiang Province, Hangzhou 310016, China

<sup>4</sup>School of Environment, School of Marine Science and Technology (Weihai), Harbin Institute of Technology, Weihai 150090, China

\*Corresponding Authors

Prof. Bin Su

Email: subin@zju.edu.cn

## Table of Contents

S1. Illustration of the ECL Analytical System	S-3
S2. Electrochemical Reduction of O <sub>2</sub>	S-4
S3. Variation of ECL Intensity upon Addition of Radical Scavengers	S-5
S4. Effect of Radical Scavengers on ORR	S-6
S5. ECL Curves Obtained with Different Concentrations of L012	S-7
S6. ECL Spectrum of the Cathodic System	S-8
S7. Intermediates of L012 During ECL Reactions	S-9
S8. Calculation of Rate Constants	S-10
S9. UV-visible Absorbance Spectra of Juice Samples	S-13
References	S-14

## S1. Illustration of the ECL Analytical System

As shown in **Fig. S1**, the custom ECL analysis system used for measuring ECL intensity consisted of an electrochemical workstation (CHI 832C, CH Instrument), a counting unit (Hamamatsu, C8805-01) and a photon counting detector (Hamamatsu, CH277).<sup>S1</sup>

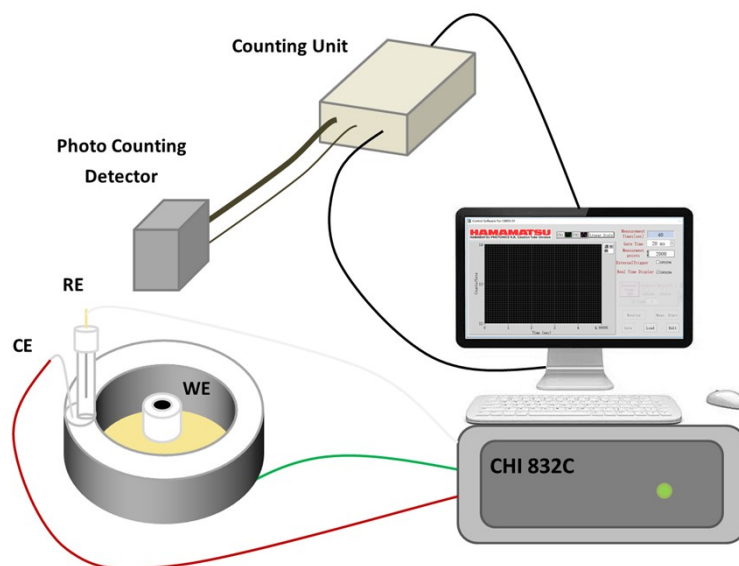


**Fig. S1** Illustration of the custom upright ECL analytical system.

## S2. Electrochemical Reduction of O<sub>2</sub>

Fig. S2 displays the variation of linear scan voltammetry (LSV) curves of GCE in O<sub>2</sub>-saturated PB solution with the scan rate. The magnitude of peak current is linearly related with the square root of scan rate, suggesting the electrochemical reduction of O<sub>2</sub> at GCE surface is diffusion-controlled.

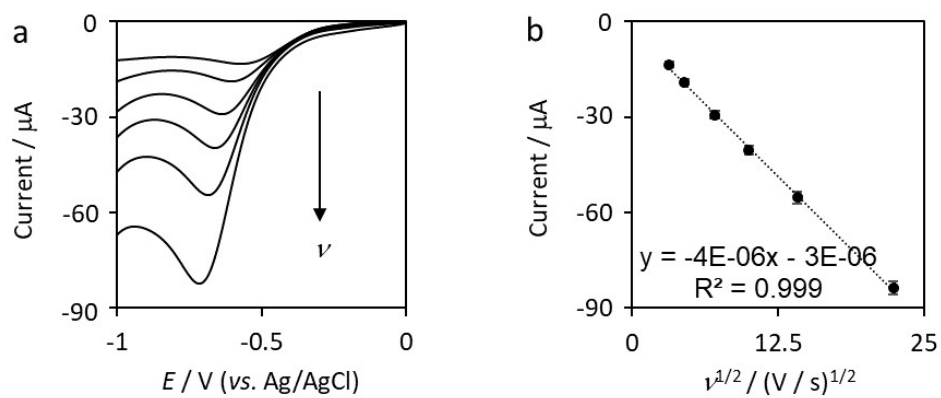
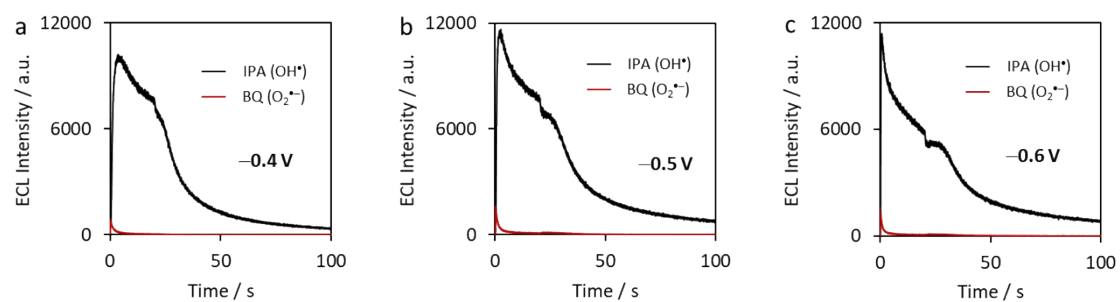


Fig. S2 (a) LSV curves in O<sub>2</sub>-saturated PB solution (0.2 M, pH = 7.0). The scan rate was varied from 10 to 200 mV s<sup>-1</sup>. (b) The relationship between peak current and square root of the scan rate.

### S3. Variation of ECL Intensity upon Addition of Radical Scavengers



**Fig. S3** Variation of ECL intensity at different potentials in O<sub>2</sub>-saturated PB solution (0.2 M, pH 7.0) containing 100  $\mu$ M L012 upon the addition of BQ (50  $\mu$ M) and IPA (10 mM) as the radical scavenger. The potential was applied for 20 s.

#### S4. Effect of Radical Scavengers on ORR

As shown in **Fig. S4**, CVs of GCE in IPA solution are almost the same with those in blank PB solution, indicating that the addition of IPA barely affected the electroreduction of  $O_2$  at GCE. As for BQ, a pair of redox peaks were observed, resulting from the redox reaction of BQ. Nevertheless, the magnitude of the redox peaks was much smaller than that of oxygen reduction peak at ca.  $-0.7$  V and the redox peak potential of BQ was much positive than that of oxygen reduction. Therefore, the effect of BQ on the electroreduction of  $O_2$  at GCE was negligible.

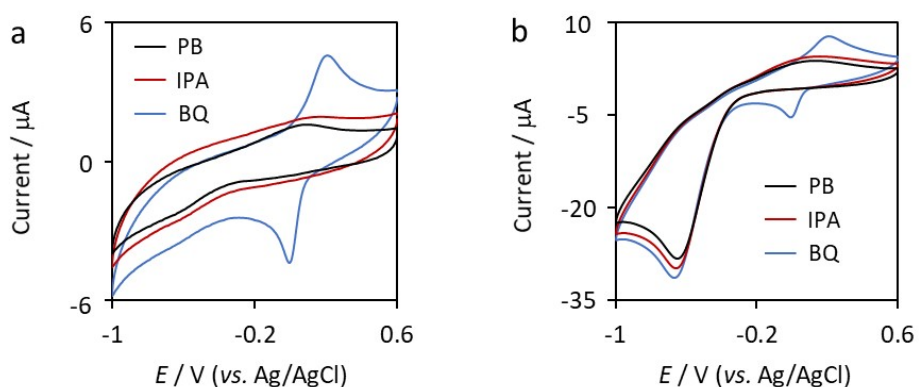


**Fig. S4** CVs of GCE in (a) Ar-saturated and (b)  $O_2$ -saturated PB solution (0.2 M, pH = 7.0) without and with the radical scavengers. The concentrations of BQ and IPA were 50  $\mu M$  and 10 mM, respectively. The scan rate was 0.1 V/s.

## S5. ECL Curves Obtained with Different Concentrations of L012

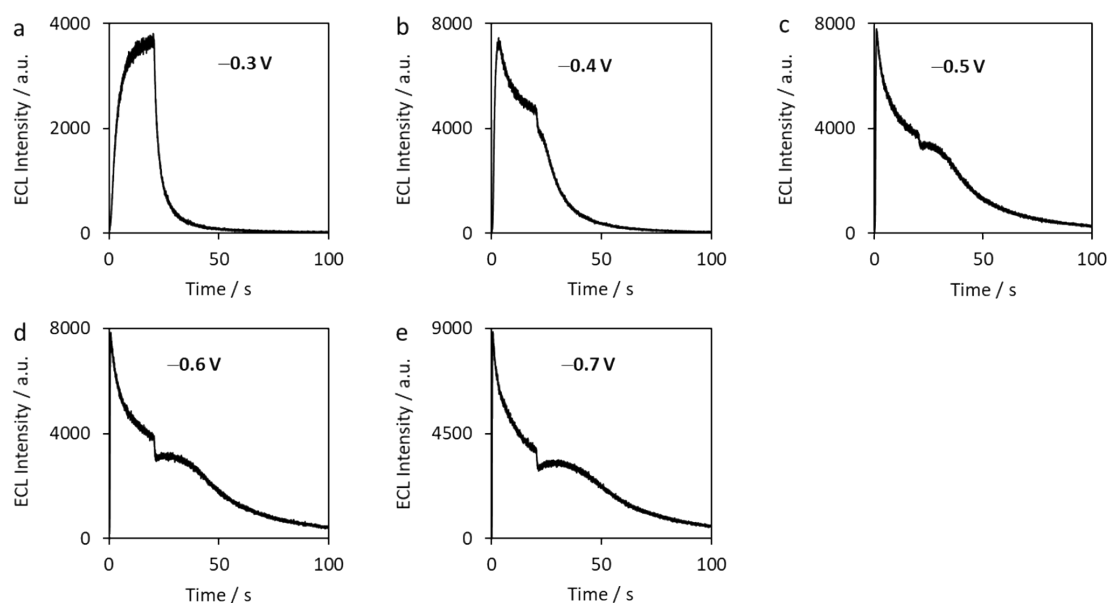


**Fig. S5** Variation of ECL intensity with time at different applied potentials in PB solution (0.2 M, pH 7.0) containing 50 μM L012: -0.3 V (a, b), -0.4 V (c), -0.5 V (d), -0.6 V (e), -0.7 V (f). The potential was applied for 20 s. The solutions were saturated with O<sub>2</sub>.

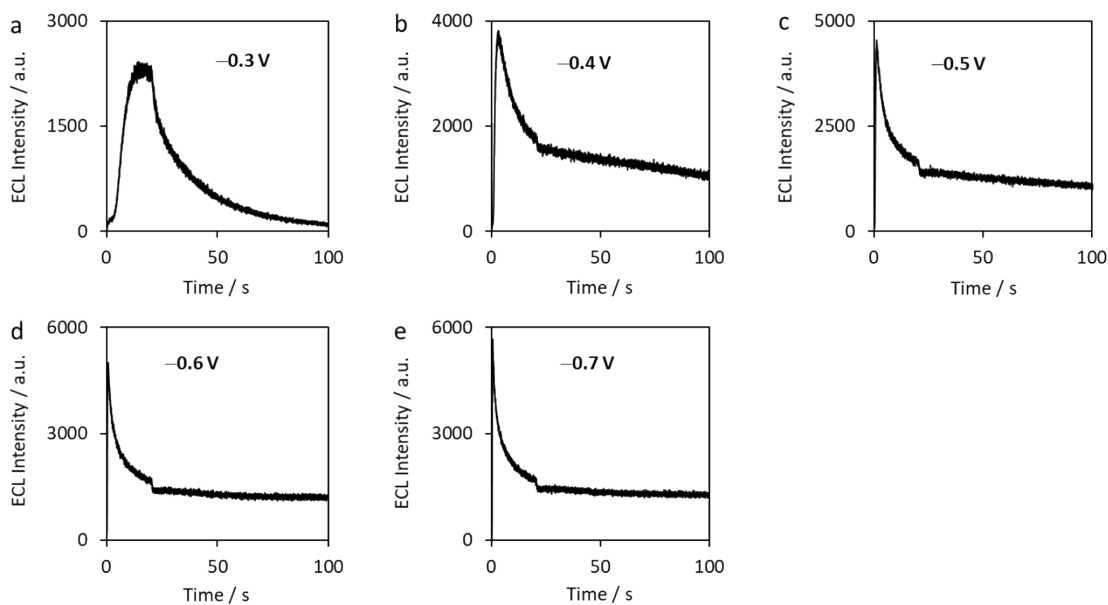


**Fig. S6** Variation of ECL intensity with time at different applied potentials in PB solutions (0.2 M, pH 7.0) containing 10 μM L012: -0.3 V (a, b), -0.4 V (c), -0.5 V (d), -0.6 V (e), -0.7 V (f). The potential was applied for 20 s. The solutions were saturated with O<sub>2</sub>.

## S6. ECL Spectrum of the Cathodic System

The ECL spectrum of the cathodic system was recorded by an optic fiber spectrophotometer (QEpro, Ocean Optics). Restricted by the sensitivity of the spectrophotometer, a GCE with diameter of 6 mm and a potential of  $-1$  V was used to enhance the signal-to-background ratio of the spectrum. The ECL spectrum is similar to those of L012 reported in the literature,<sup>S2-S4</sup> indicating that the ECL emission was originated from L012.

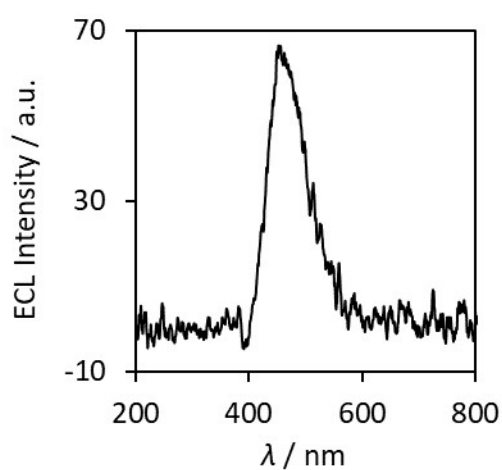


**Fig. S7** ECL spectrum obtained with a GCE electrode in  $O_2$ -saturated PB solution (0.2 M, pH 7.0) containing 100  $\mu$ M L012. The applied potential was  $-1$  V. Spectral integration time was 10 s.

## S7. Intermediates of L012 During ECL Reactions

The reactants involved in the L012 cathodic ECL process were explored by electrochemistry coupled mass spectrometry (EC-MS) to confirm the mechanism proposed in Fig. 4. The EC-MS is composed of an electrochemical flow cell, an easy ambient sonic-spray ionization (EASI) source, a heating tube and a mass spectrometer. The potential was applied by a CHI 660E electrochemical workstation (Chenhua, China) in a three-electrode configuration, where glassy carbon electrode, Ag/AgCl electrode and platinum plate were utilized as WE, RE and CE, respectively. WE and CE were positioned on the left side and right side of the electrochemical flow cell, respectively.<sup>51, 55</sup> And the reduction potential applied was  $-2$  V. In the experiments, the sample solution was injected into the flow cell at a constant rate of  $25 \mu\text{L min}^{-1}$ . The pressure of nitrogen gas was set at 60 psi and the temperature of heating tube was kept at  $100$  °C. The solution used for MS experiments was the mixture of  $0.2$  mM phosphate buffer (PB, pH 7.0) and acetonitrile ( $V:V = 1:1$ ) containing  $100$  ppm L012. All MS data were obtained under negative-ion mode using an LTQ mass spectrometer (Thermo Fisher Scientific, Waltham, MA, USA). And the Xcalibur software package was used to analyze the data. The capillary temperature, capillary voltage and tube lens voltage were kept at  $275$  °C,  $35$  V and  $110$  V, respectively. The collision induced dissociation was set as  $30$  V or  $35$  V. The maximal ion injection time was  $30$  ms.

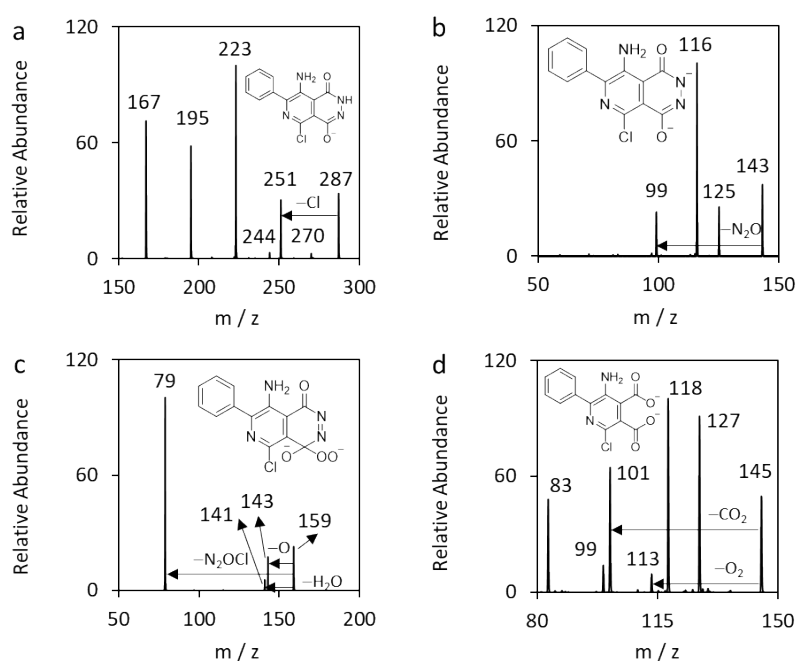


Fig. S8 MS<sup>2</sup> spectra of (a) LH, (b) L<sup>-</sup>, (c) LO<sub>2</sub><sup>2-</sup> and (d) AP<sup>2-</sup>.

## S8. Calculation of Rate Constants

In the potential range from  $-0.43$  V to  $-0.45$  V,  $k_1$  can be estimated according to the Butler-Volmer Equation,<sup>S6-S8</sup>

$$-j = j_0 \exp\left[-\alpha \frac{nF}{RT}(E - E_0)\right] \quad (\text{S1})$$

$$E - E_0 = \frac{2.3RT}{\alpha nF} \log j_0 - \frac{2.3RT}{\alpha nF} \log(-j) \quad (\text{S2})$$

$$j_0 = nFk_0 [\text{O}_2] \quad (\text{S3})$$

$$k = k_0 \exp\left[-\alpha \frac{nF}{RT}(E - E_0)\right] \quad (\text{S4})$$

where  $j$  and  $j_0$  represent the cathodic current density and exchange current density.  $F$ ,  $R$  and  $T$  are the Faraday constant, gas constant and temperature, respectively. The bulk concentration of dissolved oxygen is about  $1.3$  mM.<sup>S9</sup>  $k_0$  and  $E_0$  are the standard rate constant of electrochemical reduction and the standard redox potential. The surface area of GCE was  $0.071$  cm<sup>2</sup>. Thus, the current density due to the reduction of  $\text{O}_2$  was obtained from **Fig. S8a** and **b**. When the overpotential ( $E - E_0$ ) is larger than  $0.1$  V, the Butler-Volmer equation can be simplified as eq. S1. Thus,  $j_0$  and  $\alpha$  can be evaluated from the intercept and slope of the linear curve (**Fig. S8c**). Thus,  $k_0$  was obtained according to eq. S3. Finally, the rate constant at  $-0.3$  V was calculated to be  $5.2 \times 10^{-4}$  cm s<sup>-1</sup> according to eq. S4. If assuming an electron transfer distance of ca.  $1$  nm, it amounts to a first order rate constant of  $5.2 \times 10^3$  s<sup>-1</sup> ( $k_1$ ).

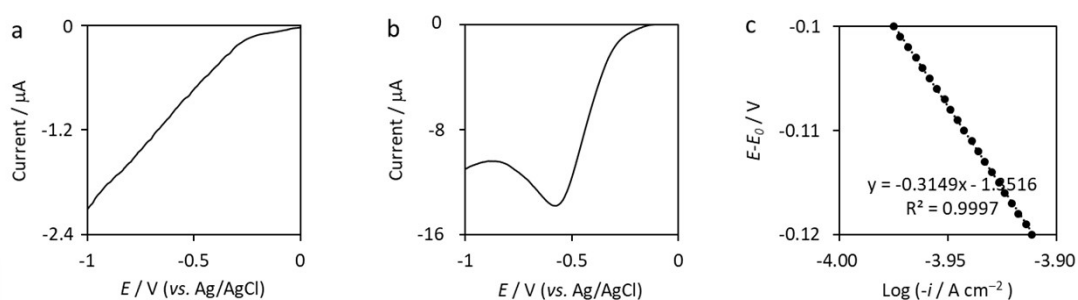


**Fig. S9** (a) LSV curve in Ar-saturated PB solution (0.2 M, pH = 7.0). (b) LSV curve in PB solution (0.2 M, pH = 7.0). (c) The relationship between  $E - E_0$  and the logarithm of the current intensities in the potential range from  $-0.43$  V to  $-0.45$  V.  $E_0$  is the standard redox potential for  $\text{O}_2^*$ . The scan rate was  $0.01$  V/s.

The average concentration of  $O_2^{\bullet-}$  generated during ECL reactions can be obtained according to eqs. S5-8. First, the amount of  $O_2^{\bullet-}$  ( $n$ ) generated during ECL reaction was obtained from the integrated current in **Fig. S9c**,

$$n = \frac{\int_0^t i dt}{zF} \quad (S5)$$

where  $i$ ,  $t$  and  $z$  represent the current, time and electron transfer number, respectively. The diffusion length ( $L$ ) of  $O_2^{\bullet-}$  at time  $t$  can be calculated by,<sup>S10</sup>

$$L = (\pi Dt)^{\frac{1}{2}} \quad (S6)$$

where  $D$  is the diffusion coefficient of  $O_2^{\bullet-}$ . Since the surface area ( $S$ ) of GCE was known (0.071 cm<sup>2</sup>), the volume of the diffusion layer ( $V$ ) was obtained,

$$V = LS \quad (S7)$$

Finally, the concentration of  $O_2^{\bullet-}$  ( $[O_2^{\bullet-}]$ ) is calculated to be 433  $\mu$ M according to eq. S8,

$$[O_2^{\bullet-}] = \frac{n}{V} \quad (S8)$$

According to eqs. S4-5, the concentration change of  $O_2^{\bullet-}$  can be expressed as,

$$\frac{d[O_2^{\bullet-}]}{dt} = k_1[O_2] - k_2[L^-][O_2^{\bullet-}]^2 \quad (S9)$$

where  $[O_2]$  and  $[L^-]$  are the concentrations of  $O_2$  and  $L^-$ , respectively. Further assuming that the generation and consumption of  $O_2^{\bullet-}$  is equal at  $-0.3$  V, namely the variation of  $[O_2^{\bullet-}]$  is zero, we have,

$$k_2 = \frac{k_1[O_2]}{[L^-][O_2^{\bullet-}]^2} \quad (S10)$$

Since concentrations of  $O_2$ ,  $L^-$  and  $O_2^{\bullet-}$  are 1.3 mM, 0.1 mM and 0.433 mM, respectively, the value of  $k_2$  was calculated to be  $3.61 \times 10^{11} \text{ M}^{-2} \text{ s}^{-1}$ .

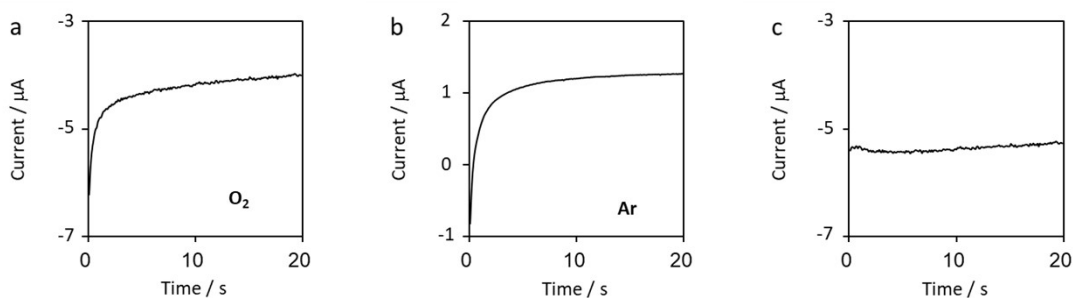


**Fig. S10** (a, b)  $i$ - $t$  curves of GCE in (a)  $O_2^-$  and (b) Ar-saturated PB solutions (0.2 M, pH 7.0) containing 100  $\mu$ M L012. (c)  $i$ - $t$  curve obtained by subtracting  $i$ - $t$  curve in (b) from that in (a). The applied potential was  $-0.3$  V.

According to eqs. S5-6, the concentration variation of  $\text{LO}_2^{2-}$  can be obtained by eqs. S11-13,

$$\frac{d[\text{LO}_2^{2-}]}{dt} = k_2[\text{L}^-][\text{O}_2^{*-}]^2 - k_3[\text{LO}_2^{2-}] = k_1[\text{O}_2] - k_3[\text{LO}_2^{2-}] \quad (\text{S11})$$

$$\int_0^{[\text{LO}_2^{2-}]} \frac{d[\text{LO}_2^{2-}]}{k_1[\text{O}_2] - k_3[\text{LO}_2^{2-}]} = \int_0^t dt \quad (\text{S12})$$

$$[\text{LO}_2^{2-}] = \frac{k_1[\text{O}_2]}{k_3}(1 - e^{-k_3 t}) \quad (\text{S13})$$

Accordingly, the variation of ECL intensity with time was obtained,

$$I_{\text{ECL}} = \varphi_{\text{ECL}} \frac{d[h\nu]}{dt} = \varphi_{\text{ECL}} k_3 [\text{LO}_2^{2-}] = \varphi_{\text{ECL}} k_1 [\text{O}_2] (1 - e^{-k_3 t}) \quad (\text{S14})$$

Finally, the value of  $k_3$  was calculated to be  $0.19 \text{ s}^{-1}$  by fitting experimental curves using eq. S14.

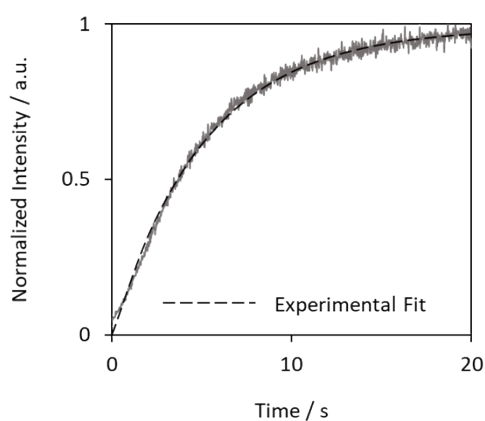


**Fig. S11** Experimental (solid) and simulated (dotted) normalized ECL intensity-time curves at  $-0.3 \text{ V}$ . The data in **Fig. 2a** was used.

## S9. UV-visible Absorbance Spectra of Juice Samples

The commercial juices were purified by a 0.22  $\mu\text{m}$  filter prior to use. And then they were diluted by 100 times with PB solution (0.2 M, pH = 7.0), without any further complex treatment. The absorbance spectra of juice samples were recorded by an optic fiber ultraviolet-visible (UV-visible) spectrophotometer (QEpro, Ocean Optics).

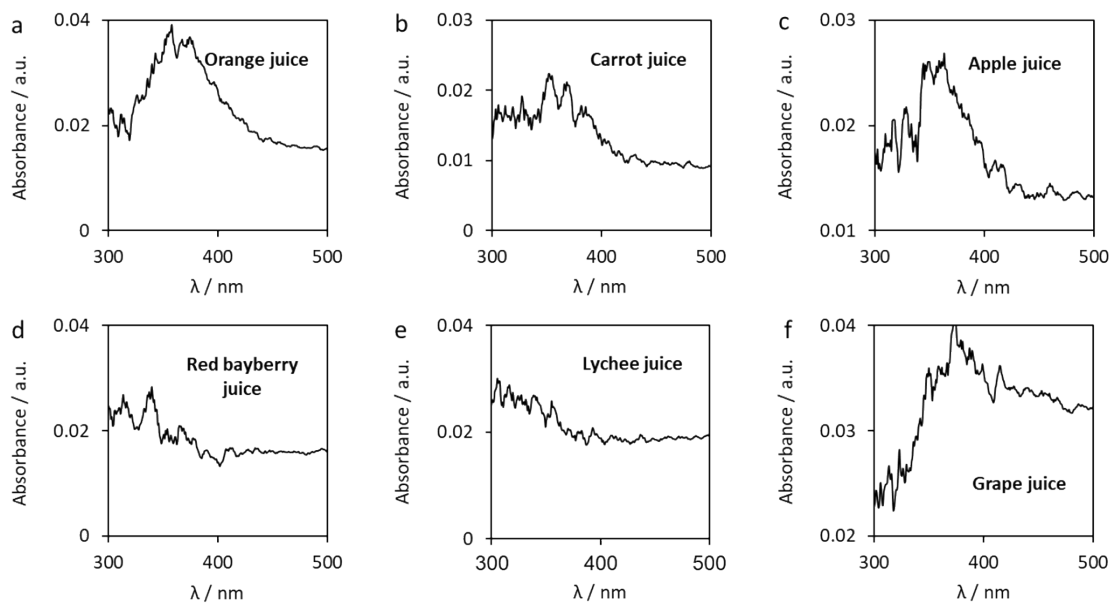


**Fig. S12** UV-visible absorbance spectra of the juice samples.

## References

- S1. Y. Wang, J. Ding, P. Zhou, J. Liu, Z. Qiao, K. Yu, J. Jiang, B. Su, *Angew. Chem. Int. Ed.*, 2023, **62**, e202216525.
- S2. J. Zielonka, J. D. Lambeth, B. Kalyanaraman, *Free Radical Biol. Med.*, 2013, **65**, 1310-1314.
- S3. M. Feng, A. L. Dauphin, L. Bouffier, F. Zhang, Z. Wang, N. Sojic, *Anal. Chem.*, 2021, **93**, 16425-16431.
- S4. W. Wang, X. Wu, K. W. Kevin Tang, I. Pyatnitskiy, R. Taniguchi, P. Lin, R. Zhou, S. L. C. Capocyan, G. Hong, H. Wang, *J. Am. Chem. Soc.*, 2023, **145**, 1097-1107.
- S5. J. Jiang, Z. Hong, Z. Qiao, Q. Zhu, H. Zhang, Y. Jiang, K. Yu, *J. Electroanal. Chem.*, 2023, **932**, 117248.
- S6. A. J. Bard, L. R. Faulkner, *Electrochemical methods: Fundamentals and applications*, Wiley, New York, 2 edn., 2002.
- S7. M.-M. Chen, C.-H. Xu, W. Zhao, H.-Y. Chen, J.-J. Xu, *Chem. Commun.*, 2020, **56**, 3413-3416.
- S8. J. Ding, P. Zhou, B. Su, *ChemElectroChem*, 2022, **9**, e202200236.
- S9. W. H. Koppenol, J. Butler, *Adv. Free Radical Biol. Med.*, 1985, **1**, 91-131.
- S10. Y. Koizumi, Y. Nosaka, *J. Phys. Chem. A*, 2013, **117**, 7705-7711.